

## OXIDATION KINETICS AND MICROSTRUCTURE OF V-(4-5) WT.%Cr-(4-5) WT.%Ti ALLOYS EXPOSED TO AIR AT 300-650°C\*

K. Natesan (Argonne National Laboratory) and M. Uz (Lafayette College, Easton, PA)

### OBJECTIVE

The objectives of this task are to (a) evaluate the oxygen uptake of V-Cr-Ti alloys as a function of temperature and oxygen partial pressure in the exposure environment, (b) examine the microstructural characteristics of oxide scales and oxygen trapped at the grain boundaries in the substrate alloys, and (c) evaluate the influence of oxygen uptake on the tensile properties of the alloys at room and elevated temperatures.

### SUMMARY

A systematic study was conducted to determine the effects of time and temperature of air exposure on the oxidation behavior and microstructure of V-4Cr-4Ti (44) and V-5Cr-5Ti (55) alloys. All samples were from 1-mm-thick cold-rolled sheets, and each was annealed in vacuum at 1050°C for 1 h prior to high-temperature exposure. Different samples from each alloy were heated in ambient air at 500°C for times ranging from 24 to ≈2000 h, and in a thermogravimetric analysis (TGA) apparatus at 300 to 650°C. Models describing the oxidation kinetics, the oxide type and its thickness, alloy grain size, and the depth of oxygen diffusion in the substrate alloy were determined for the two alloys and compared. The results showed that the oxide layers that formed on the surfaces of both alloys in air in the temperature range of 300-650°C are protective, and that the 55 alloy is slightly more oxidation-resistant than the 44 alloy.

### EXPERIMENTAL PROGRAM

The 44 and 55 alloys were obtained as 1-mm-thick cold-rolled sheets. Samples with dimensions of about 1 x 10 x 20 mm were cut from each alloy. Before any further treatment or testing, all samples were annealed for 1 h at 1050°C under a pressure of  $\approx 10^{-6}$  torr. The samples were wrapped in tantalum foil to protect them from contamination during this heat treatment process. Samples from each alloy were analyzed for chemical composition before and after annealing, and the results can be seen in Table 1. As shown, the total amount of other impurities in either alloy was less than 0.3%, with silicon (Si) as the major impurity at  $\approx 0.08\%$ .

Samples from the 44 and 55 alloys were heated in air at 500°C for about 24, 250, 600, 1050, and 2100 h to study the effects of time on their oxidation behavior. Samples from each alloy were also heated in a TGA apparatus in air at different temperatures to determine oxidation kinetics as a function of temperature. The TGA experiments were carried out at 320, 400, 500, 575, and 620°C for the 44 samples, and at 300, 400, 500, 575, and 650°C for the 55 samples. Weight gain was recorded continuously on a strip chart throughout each experiment.[1,2] All samples were also weighed separately before and after any high-temperature exposure to determine the resulting total weight change.

The oxide scales on the samples were identified by X-ray diffraction (XRD) analysis on the surfaces of several samples, as well as on the oxides scraped from their surfaces. Oxide residues obtained from the 44 and 55 alloys exposed to air at 500°C for 2100 h by dissolving away the matrix were analyzed for the V, Cr, and Ti using the inductively coupled plasma (ICP) technique. A 900 mL methanol-100 mL bromine-10 g tartaric acid was used for phase extraction with platinum wire as the catalyst. Metallographic examination of the longitudinal and transverse cross-sections of the cold-rolled and thermally treated samples used both an optical microscope and a scanning electron microscope (SEM).

The metallographic specimens were chemically etched with a solution of lactic-nitric-hydrofluoric acids at a volume ratio of 30-15-5. The grain size of each sample exposed to high temperature (annealed or air-oxidized) was determined by both lineal and areal analysis methods according to ASTM Standard E112, and

---

\*This work has been supported by the U.S. Department of Energy, Office of Fusion Energy Research, under Contract W-31-109-Eng-38.

the average of the two was reported as the grain size of each sample. Oxygen diffusion depth (or the depth of the hardened layer) of each oxidized sample was estimated from the microhardness profile along its thickness, which was obtained with a Vickers microhardness tester and a load of 25-50 g. Furthermore, the oxygen profiles of several samples were determined by secondary ion mass spectroscopy (SIMS) line profiles along the thickness to verify the results obtained by the microhardness measurements.

All data in this study were processed and analyzed with a spreadsheet program capable of graphical, statistical, and regression analyses.

## RESULTS AND DISCUSSION

The results of the TGA experiments (carried out to determine the oxidation behavior of the 44 and 55 alloys in the temperature range of 300-650°C) are tabulated in Table 1, with the sample and the oxidation temperature given in columns 1 and 2, respectively. In column 3, the first equation at each temperature represents the oxidation model that best fit the experimental data. The second equation represents the parabolic model and provides a more conservative rate constant (coefficient of time) at that temperature. In the first two equations,  $w_f$  and  $w_p$  have the units of  $\text{mg}\cdot\text{mm}^{-2}$ , and time  $t$  is in hours (h). The third equation in column 3 at each temperature,  $x$  with units of  $\text{mm}^2\cdot\text{h}^{-1}$ , was obtained by dividing the first equation by the square of density which is  $3.357\text{ g}\cdot\text{cm}^{-3}$  (or  $\text{mg}\cdot\text{mm}^{-3}$ ), and is provided to allow ready estimation of the scale thickness,  $x$ , for any desired time at each temperature. The coefficient of time ( $t$ ) in each equation is the rate constant (denoted by  $k$  in general, and by  $k_f$ ,  $k_p$  or  $k_x$  depending on the models described in Table 1) at the corresponding temperature with the units as indicated.

No measurable weight gain was observed in the 55 alloy oxidized at 300°C. The TGA data for the 44 and 55 alloys are presented in Fig. 1 as plots of weight gain versus time. In these plots, the lines represent the oxidation models that best fit the experimental data, which are shown as circles for the 44 samples and as squares for the 55 samples. The results show that in both alloys, oxidation (scale growth) occurs according to a nonlinear growth rate law, and the rate of oxidation decreases with time, indicating a protective oxide scale. Together with the lack of spalling of the scale, these results provide evidence that  $\text{V}_2\text{O}_5$  forms as a nonporous and tenacious oxide on the surface of 44 and 55 alloys in the temperature range of 350-650°C. As can be seen from the plots in Fig. 1, oxidation rate increased with increasing temperature. As expected, the temperature-dependence of the rate constant was in Arrhenius form, and the data for both alloys fit well an equation of the form

$$k = k_0 \exp[Q_{\text{Ox}}/(RT)], \quad (1)$$

where  $k$  is the rate constant, ( $k_f$ ,  $k_p$  or  $k_x$ ),  $k_0$  is the pre-exponential constant,  $Q_{\text{Ox}}$  is the activation energy for the oxidation process, and  $R$  and  $T$  are the gas constant and absolute temperature, respectively. The Arrhenius plots for the 44 and 55 alloys are shown in Fig. 2, which indicates little difference between the rate constants at a given temperature and the slope of the line for the two alloys, with those for the 44 slightly higher. While the oxide that forms on both alloys is predominantly  $\text{V}_2\text{O}_5$ , the slightly higher oxidation resistance of the 55 alloy is attributable to its slightly higher substitutional alloying content, especially Ti, which is known to trap oxygen and slow its diffusion in the matrix. This may also be due to the larger average grain size of the 55 alloy, which means less grain boundary area and thus allowing a fast transport path for oxygen. The activation energies for the air-oxidation process as determined from Fig. 2 were about 135 kJ/mol for the 44 alloy and 130 kJ/mol for the 55 alloy.

Oxidation rate constants, and data for diffusion of O in V and its alloys with Cr and/or Ti and in  $\text{V}_2\text{O}_5$ , are tabulated in Table 2, data sources are identified. The rate constants for the 44 and 55 alloys in column 2 were obtained from the variation of the measured oxide scale thickness with time, and those in column 3 are from the oxidation models developed from the TGA results. Data for oxygen diffusion in V and its alloys, as well as in the oxides that form on them, are given in columns 4-7 of the table; values for the 44 and 55 alloys are from this work, and those for others are from the literature as indicated. The diffusion coefficients,  $D$ , of O in the 44 and 55 alloys were determined from the oxygen diffusion distance-time data assuming one-dimensional diffusion, which should be valid on the basis of the geometry of the samples

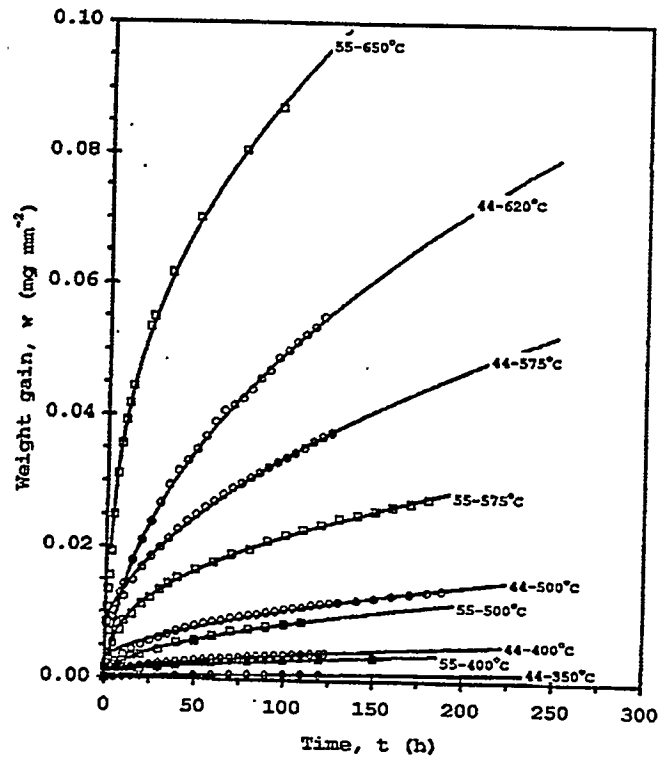


Fig. 1 Variation of weight gain with time in air for 44 and 55 alloys. At each temperature, data points are from TGA experiments, and solid lines represent model that best describes the oxidation behavior of the alloy

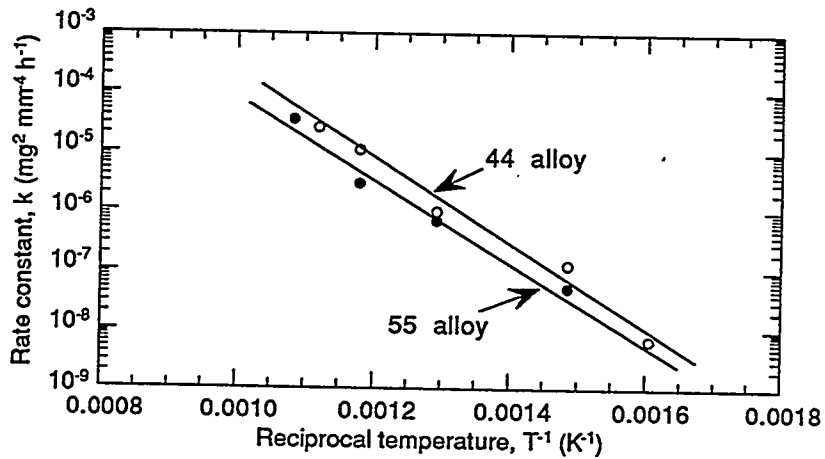


Fig. 2 Arrhenius plots of oxidation rate constants for 44 and 55 alloys exposed to air at temperatures up to 650°C

Table 1. Mathematical models describing oxidation behavior of V-4 wt.%Cr-4 wt.%Ti (44) and V-5 wt.%Cr-5 wt.%Ti (55) alloys as obtained using data from TGA experiments.<sup>a</sup>

Alloy	T (°C)	Oxidation model	R <sup>2</sup>
44	350	$w_f^2 = -1.77 \times 10^{-8} + 6.76 \times 10^{-9} t$	0.999
		$w_p^2 = 6.54 \times 10^{-9} t$	0.997
		$x^2 = -1.57 \times 10^{-9} + 6.00 \times 10^{-10} t$	
44	400	$w_f^2 = 1.31 \times 10^{-6} + 1.28 \times 10^{-7} t$	0.999
		$w_p^2 = 1.43 \times 10^{-7} t$	0.984
		$x^2 = 1.16 \times 10^{-7} + 1.14 \times 10^{-8} t$	
44	500	$w_f^2 = 1.17 \times 10^{-5} + 9.82 \times 10^{-7} t$	1.0
		$w_p^2 = 1.08 \times 10^{-6} t$	0.992
		$x^2 = 1.04 \times 10^{-6} + 8.71 \times 10^{-8} t$	
44	575	$w_f^2 = 7.81 \times 10^{-5} + 1.07 \times 10^{-5} t$	1.0
		$w_p^2 = 1.16 \times 10^{-5} t$	0.998
		$x^2 = 6.93 \times 10^{-6} + 9.50 \times 10^{-7} t$	
44	620	$w_f^2 = -5.40 \times 10^{-5} + 2.54 \times 10^{-5} t$	1.0
		$w_p^2 = 2.48 \times 10^{-5} t$	0.998
		$x^2 = -4.79 \times 10^{-6} + 2.25 \times 10^{-6} t$	
55	†300		
55	400	$w_f^2 = -3.88 \times 10^{-7} + 4.13 \times 10^{-7} t^{1/2} + 5.23 \times 10^{-8} t$	0.999
		$w_p^2 = 8.90 \times 10^{-8} t$	0.997
		$x^2 = -3.44 \times 10^{-8} + 3.67 \times 10^{-8} t^{1/2} + 4.64 \times 10^{-9} t$	
55	500	$w_f^2 = 1.16 \times 10^{-8} + 7.02 \times 10^{-7} t$	0.999
		$w_p^2 = 7.07 \times 10^{-7} t$	0.977
		$x^2 = 1.03 \times 10^{-9} + 6.23 \times 10^{-8} t$	
55	575	$w_f^2 = -1.78 \times 10^{-5} + 2.02 \times 10^{-5} t^{1/2} + 2.94 \times 10^{-6} t$	1.0
		$w_p^2 = 4.59 \times 10^{-6} t$	0.986
		$x^2 = -1.58 \times 10^{-6} + 1.79 \times 10^{-6} t^{1/2} + 2.61 \times 10^{-7} t$	
55	650	$w_f^2 = -3.77 \times 10^{-4} + 4.88 \times 10^{-4} t^{1/2} + 3.48 \times 10^{-5} t$	0.998
		$w_p^2 = 8.99 \times 10^{-5} t$	0.946
		$x^2 = -3.35 \times 10^{-5} + 4.33 \times 10^{-5} t^{1/2} + 3.09 \times 10^{-6} t$	

<sup>a</sup>The three equations at each temperature correspond to best fit of the experimental data, parabolic model, and scale thickness.

†No measurable weight gain was observed for this specimen.

The last column indicates the degree of fit obtained from the regression analysis of data.

Table 2. Rate constants for oxidation of V and V-4 wt.%Cr-4 wt.%Ti (44) and V-5 wt.%Cr-5wt.%Ti (55) alloys, and calculated values of diffusion coefficients at 500°C, and activation energies of diffusion of oxygen in V<sub>2</sub>O<sub>5</sub> under conditions indicated.

Alloy <sup>a</sup>	T (°C)	pO <sub>2</sub> (torr)	Oxide	Rate constant <sup>b</sup> (mg <sup>2</sup> ·mm <sup>-4</sup> ·h <sup>-1</sup> ) (k x 10 <sup>9</sup> )	D <sup>c</sup> (m <sup>2</sup> ·h <sup>-1</sup> ) (D x 10 <sup>15</sup> )	Q <sub>D</sub> <sup>d</sup> (kJ·mol <sup>-1</sup> )
V	450	760	V <sub>2</sub> O <sub>5</sub>	201	497	174.4
V	500	7.6	VO <sub>2</sub>	367	56.9	193.6
V	500	760	V <sub>2</sub> O <sub>5</sub>	2740	630	164.7
V	550	3	VO <sub>2</sub>	918	142	202.7
V	550	9	VO <sub>2</sub>	1920	297	194.3
V	550	36	VO <sub>2</sub>	2100	338	192.8
V	550	760	V <sub>2</sub> O <sub>5</sub>	8530	1980	172.0
V	600	1	VO <sub>2</sub>	2880	446	209.7
V	600	4	VO <sub>2</sub>	6160	954	200.1
V	600	7.6	VO <sub>2</sub>	7420	1150	197.8
V	600	760	V <sub>2</sub> O <sub>5</sub>	19600	4500	179.9
V	650	0.76	VO <sub>2</sub>	4790	742	224.5
V	650	7.6	VO <sub>2</sub>	10800	1680	213.1
44	350	160	V <sub>2</sub> O <sub>5</sub>	6.76	1.6	165.6
44	400	160	V <sub>2</sub> O <sub>5</sub>	128	29.3	161.0
44	500	160	V <sub>2</sub> O <sub>5</sub>	982	225	178.0
44	575	160	V <sub>2</sub> O <sub>5</sub>	10700	2460	179.0
44	620	160	V <sub>2</sub> O <sub>5</sub>	25400	5830	184.0
55	400	160	V <sub>2</sub> O <sub>5</sub>	52.3	12	168.4
55	500	160	V <sub>2</sub> O <sub>5</sub>	702	161	181.7
55	575	160	V <sub>2</sub> O <sub>5</sub>	2940	673	194.0
55	650	160	V <sub>2</sub> O <sub>5</sub>	34780	7980	191.0

<sup>a</sup>Data on V are from Ref. 3, and those on 44 and 55 are from this study.

<sup>b</sup>Rate coefficients for V are coefficients of time in a parabolic oxide growth rate model, and those for 44 and 55 alloys are coefficients of time in oxidation models that best fit the data in Table 1.

<sup>c</sup>Calculated at 500°C with rate constants in Table 2.

<sup>d</sup>Calculated with D values in Table 2.

used in this study. Using these diffusion coefficients, we calculated the activation energies of diffusion of oxygen in these alloys. The good agreement between the rate constant calculated from the measured data and that from the model for both the 44 and 55 alloys indicates once again that the models developed in this study describe the oxidation behavior of these alloys rather well. The diffusion coefficients were greater for oxygen diffusion in the 44 alloy than in the 55 alloy, and their magnitudes were between those of the V-5Cr and V-5Ti alloys. The activation energy of oxygen diffusion was, as expected, greater for the 55 alloy than for the 44 alloy. However, the activation energies of oxygen diffusion in both alloys were greater than those in unalloyed V and V-5Cr alloy, but considerably lower than that in V-5Ti alloy. These trends may be attributed to the binding or trapping of O by the Ti atoms that are in solid solution. On the other hand, the activation energies for the diffusion of oxygen in the oxides that formed on V and on the 44 and 55 alloys were within 10% of one another. This strongly indicates that the oxides that formed on these

materials were similar in nature, namely  $V_2O_5$ .

#### REFERENCES

- [1] K. Natesan and W. K. Soppet, "Effect of Oxidation on Tensile Properties of a V-5Cr-5Ti Alloy," Proc. 2nd Intl. Conf. Heat-Resistant Materials, eds. K. Natesan, P. Ganesan, and G. Lai, ASM International, September 11-14, 1995, Gatlinburg, TN, 375.
- [2] K. Natesan and W. K. Soppet, "Effect of Oxygen and Oxidation on Tensile Properties of V-5Cr-5TiAlloy," J. Nucl. Mater. in press.
- [3] A. Mukherjee and S. P. Wach, J. Less-Common Metals, 92 (1983) 289.